Alnersson *et al.*
Functional Composite Materials (2023) 4:11
https://doi.org/10.1186/s42252-023-00049-9

Functional Composite Materials

RESEARCH

Open Access

3D flow and fibre orientation modelling of compression moulding of A-SMC: simulations and experimental validation in squeeze flow

Gustaf Alnersson[1,2*], Erik Lejon[2], Hana Zrida[2], Yvonne Aitomäki[3], Anna-Lena Ljung[1] and T. Staffan Lundström[1]

Abstract

Sheet Moulding Compound (SMC) based composites have a large potential in industrial contexts due to the possibility of achieving comparatively short manufacturing times. It is however necessary to be able to numerically predict both mechanical properties as well as manufacturability of parts.

In this paper a fully 3D, semi-empirical model based on fluid mechanics for the compression moulding of SMC is described and discussed, in which the fibres and the resin are modelled as a single, inseparable fluid with a viscosity that depends on volume fraction of fibres, shear strain rate and temperature. This model is applied to an advanced carbon-fibre SMC with a high fibre volume fraction (35%). Simulations are run on a model of a squeeze test rig, allowing comparison to experimental results from such a rig. The flow data generated by this model is then used as input for an Advani-Tucker type of model for the evolution of the fibre orientation during the pressing process. Numerical results are also obtained from the software 3DTimon. The resulting fibre orientation distributions are then compared to experimental results that are obtained from microscopy. The experimental measurement of the orientation tensors is performed using the Method of Ellipses. A new, automated, accurate and fast method for the ellipse fitting is developed using machine learning. For the studied case, comparison between the experimental results and numerical methods indicate that 3D Timon better captures the random orientation at the outer edges of the circular disc, while 3D CFD show larger agreement in terms of the out-of-plane component. One of the advantages of the new image technique is that less work is required to obtain microscope images with a quality good enough for the analysis.

Keywords Sheet moulding compound, Numerical modelling, High volume fraction, Method of ellipses, Machine learning

Introduction

Sheet Moulding Compound (SMC) is a class of composite materials that have the possibility to be useful in automotive industrial applications, due to the possibility of comparatively short cycle times. More recently, Advanced SMC (A-SMC) has also been introduced, the main difference compared to earlier materials being that the fibres are now carbon and the volume fraction of fibres is higher (35% and higher compared to earlier 20–25%). Another important advancement is the rapid development cycles in the automotive industry meaning that it is necessary to be able to reliably numerically predict both the manufacturability and the mechanical properties of parts. While current applications for functional composites as related to SMC are limited, any future applications where the fibres add additional functions besides the structural component

*Correspondence:
Gustaf Alnersson
gustaf.alnersson@associated.ltu.se
[1] Division of Fluid and Experimental Mechanics, Luleå University of Technology, Luleå, Sweden
[2] Gestamp Hardtech, Luleå, Sweden
[3] RISE Sicomp, Öjebyn, Sweden

will require good knowledge of fibre distribution and orientation. This may, for instance, be electrical, insulation or self-healing properties.

For the moulding process, fitted pieces of sheets consisting of fibres and resin are placed inside a heated mould. When the mould closes the SMC stack melts, flows out and fills the mould after which the resin cures and the solidified composite can be removed from the mould. Process modelling of SMC is rather complicated for a number of reasons [1]. Chief among these are the complex material properties of SMCs, the presence of high-volume fractions of fibres and the steep temperature gradients. The rheology of SMC was previously studied by, among others Lee et al. [2], Dumont and Le Corre [3–5] and Vahlund et al. [6]; while the flow itself was experimentally studied by, among others Barone and Caulk [7] and Olsson et al. [8]. The fibres and in particular their orientations will also greatly affect the mechanical properties of the parts. The focus of this work will thusly be on fibre orientation prediction. The approach used for fibre orientation is the one suggested by Folgar and Tucker [9] and Advani and Tucker [10] (see, among others, [11–13] for further methods in the same family). The squeeze test rig that is studied in the work presented here is used for determining the viscous properties of materials. This study uses the geometry to compare the results of different simulation techniques. Two different approaches are discussed here. The first approach uses Ansys CFX, a commercial general fluid mechanics modelling software for the displacement of the charge (previously discussed in [14]) where the reorientation of the fibres is modelled using self-implemented functions. The second approach uses 3DTimon, a more specialized composite modelling code where Direct Fiber Simulation (DFS) is used for the fibre orientation modelling [15]. Results from both of these approaches are compared to experimental results obtained using microscopy and a new in-house image recognition code.

Methods

General code

The movement of the charge during the compression of the mould is modelled using fluid mechanics by numerically solving the complete set of Navier-Stokes equations (see for instance Cengel and Cimbala [16]). To include the complex rheology of the SMC the viscosity of it is modelled using the semi-empirical model suggested by Kluge [17]

$$\eta = 3\eta_0\left(1 + 100f_f + 1000f_f^2\right)e^{-B\left(\frac{1}{T_0}-\frac{1}{T}\right)}\left(\frac{\dot{\epsilon}}{\dot{\epsilon}_0}\right)\left(1+\dot{\gamma}^2\right)^{\frac{n_k-1}{2}} \tag{1}$$

where η is the dynamic viscosity, f_f is the fibre volume fraction, B is a temperature constant, T is the temperature, $\dot{\epsilon}$ is the strain rate, $\dot{\gamma}$ is the shear strain rate, n_k is a power law constant, and the subscript 0 indicates initial values. Hence notice that the effect of the fibres on the flow is included in this model.

The fibre orientation evolution, in its turn, is modelled using the model suggested by Folgar and Tucker [9] and Advani and Tucker [10], in which the fibres are assumed to be rigid ellipsoidal particles with a large aspect ratio, and that they are sufficiently large so that Brownian motion can be neglected. There are a number of issues with this approach as described in [18], but the model is still applied in most commercial codes designed for composites manufacturing. Orientation tensors are used to describe the alignment with the principal axes. The time evolution of the orientation tensors may be written as

$$\frac{Da_{ij}}{Dt} = -\frac{1}{2}\left(\omega_{ik}a_{kj} - a_{ik}\omega_{kj}\right) + \frac{1}{2}\lambda\left(\dot{\gamma}_{ik}a_{kj} + a_{ik}\dot{\gamma}_{kj} - 2\dot{\gamma}_{kl}a_{ijkl}\right) + 2D_r(\delta_{ij} - \alpha a_{ij}) \tag{2}$$

where a_{ij} is the orientation tensor, ω is the vorticity, $\dot{\gamma}$ is the shear strain rate and D_r is the rotary diffusivity. An alternative to orientation tensors is quartonions [19]. These have some advantages when it comes to full rotations which is not considered to be important for the high fibre volume content suspension here studied. Worth noting is that Eq. (2) contains a fourth-order orientation tensor, which usually is handled using a closure approximation. Here the hybrid closure approximation suggested by Advani and Tucker [20] has been implemented as

$$\bar{a}_4 \cong \bar{a}_{ijkl} = (1-f)\widehat{a}_{ijkl} + f\widetilde{a}_{ijkl} \tag{3}$$

In Eq. (3), $\widehat{a}$ is the linear closure approximation according to (see also [21])

$$\widehat{a}_{ijkl} = -\frac{1}{35}\left(\delta_{ij}\delta_{kl} + \delta_{ik}\delta_{jl} + \delta_{il}\delta_{jk}\right) + \frac{1}{7}\left(a_{ij}\delta_{kl} + a_{ik}\delta_{jl} + a_{il}\delta_{jk} + a_{kl}\delta_{ij} + a_{jl}\delta_{ik} + a_{jk}\delta_{il}\right) \tag{4}$$

while $\widetilde{a}$ is the quadratic closure approximation which is described as

$$\widetilde{a}_{ijkl} = a_{ij}a_{kl}, \tag{5}$$

and f is a scalar measure of orientation that here is defined as

$$f = 1 - N\det(a_{ij}). \tag{6}$$

In Eq. (6), N varies depending on whether cases are studied in 2D or 3D, and is equal to 27 for 3D cases.

The fibre orientation modelling is directly implemented in CFX using, so called, user functions.

3DTimon

3DTimon is applied for the second numerical approach. This is a software developed by Toray Engineering for modelling of the manufacturing of plastic moulded products including fibre reinforced polymer composites. The viscosity model for all but the fibres in the SMC is in this case described in the following way

$$\eta = \frac{\eta_0}{1 + \left(\frac{\eta_0 \dot{\gamma}}{\tau^*}\right)^{1-n_t}}, \eta_0 = De^{\frac{A_1(T-T^*)}{A_2+(T-T^*)}} \tag{7}$$

with η again being the dynamic viscosity, T is the temperature, $\dot{\gamma}$ is the shear rate, n_t a power law constant, D and A_1 temperature constants, and T and A_2 factors connected to flow pressure.

For fibre orientation simulations in 3DTimon, Direct Fibre Simulation (DFS) is used [15]. In this approach, each fibre is modelled as a sequence of rigid rods, which allows for modelling of fibre bending and fibre breaking.

Experimental setup

Method of ellipses

The method of ellipse is a common experimental approach applied in many studies [22–24] to extract the orientation tensors of fibres throughout the projection of their cross section on a 2D micrograph. The fibres' cross sections are then fitted to ellipses followed by geometrical measurements of the major axis "a" and minor axis "b" length, which are used to determine the orientation angles of each fibre.

Each fibre is presented by a vector p in space as illustrated in Fig. 1:

$$\begin{aligned} \theta &= \arccos\left(\frac{b}{a}\right) \\ p_1 &= \sin(\theta)\cos(\varphi) \\ p_2 &= \sin(\theta)\sin(\varphi) \\ p_3 &= \cos(\theta) \end{aligned} \tag{8}$$

The orientation state of each fibre can be described by a probability distribution function $\Psi(\theta, \phi)$, such that

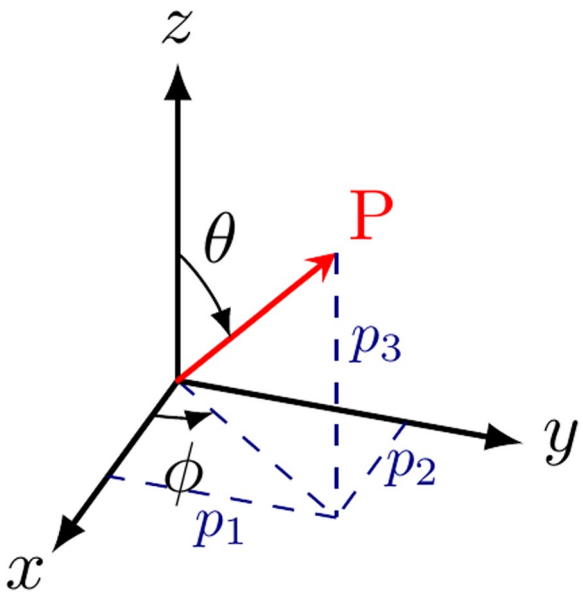

Fig. 1 A description of the coordinate system used

the probability that a fibre is in the span θ to $\theta + d\theta$, ϕ to $\phi + \mathrm{d}\phi$ is

$$\Psi(\theta, \phi)\sin\theta \mathrm{d}\theta \mathrm{d}\phi. \tag{9}$$

Since Ψ is a density function it is subject to the normalization

$$\int_{\theta=0}^{\pi}\int_{\varphi=0}^{2\pi} \Psi(\theta, \phi)\sin\theta \mathrm{d}\theta \mathrm{d}\phi = \oint \Psi(\mathbf{p})\mathrm{d}\mathbf{p} = 1 \tag{10}$$

The second order orientation tensor is calculated by a dyadic product of the vector $\mathbf{p}$ according to

$$a_{ij}^k = \frac{1}{n}\left(\sum_{k=1}^{n} p_i^k p_j^k\right), i, j = 1,2,3 \tag{11}$$

When a composite sample containing fibres with a finite length is cut, it is more likely to cut across a fibre than to cut down the length of a fibre. Therefore, a weighing function F is used to compensate for this visual bias in the calculation of the average components of the orientation tensor, such that

$$P(\theta) = L\cos(\theta) + D\sin(\theta) \tag{12}$$

and

$$a_{ij} = \frac{\sum_{k=1}^{n} F^k a_{ij}}{\sum_{k=1}^{n} F^k} \tag{13}$$

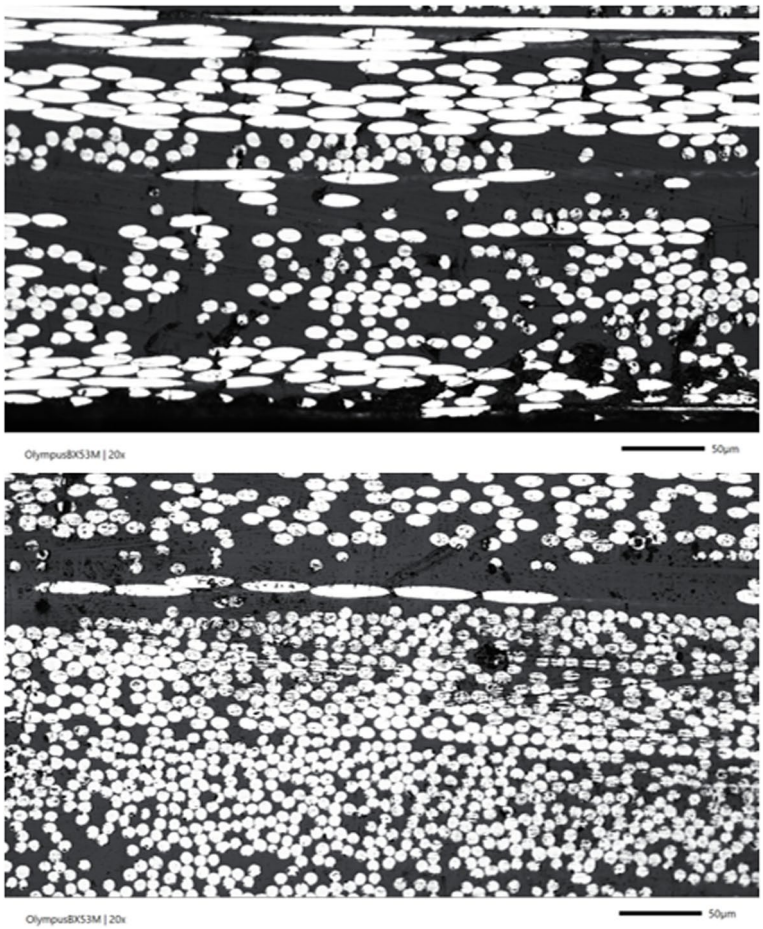

Fig. 2 Examples of microscopy images of polished cross-sections of moulded SMC. The matrix is dark grey and the fibres are the white areas

where L is fibre length, D is diameter and F^k is the inverse of Eq. (12).

The analysis applied is based on some assumptions:

- The fibres have a circular cross-section with the same diameter (being the mean diameter of all fibres). The error that may occur due to the fact that carbon fibres are not perfectly circular is neglected.
- The fibres behave as straight rods: Since they are gathered in bundles with high volume fraction and are partially entangled, this is a valid assumption.

Two fibres at angles (θ,ϕ) and $(\theta-\pi,\phi+\pi)$ cannot be distinguished from each other in the 2D micrographs (leading to the same orientation tensors). Clarke et al. [25] suggested a new technique to solve this problem, based on confocal laser scanning microscopy for improving the 3D fibres orientation study. It was successful with glass fibre composites allowing investigation of optical sections at a depth (≥ 40 μm). However, the application of this technique with carbon fibre composites is limited where the reached depth is only 5–10 μm due to the opaque nature of the fibres and the high volume fraction. In this study, the experimental measurements are limited to 2D measurements and thus it is assumed that the fibres are distributed equally between these angles, an assumption that do not influence the measured values of the orientation tensor.

Sample preparation

Using conventional computer-aided image analysis techniques, high resolution with excellent contrast is required to be able to distinguish the fibres contour and fit them to ellipses. All steps for the sample preparation, as described in [26, 27], from polishing to etching should, normally, be followed carefully. One of the advantages of the new technique applied in this study, presented in the next section, is that much less work is required to obtain microscope images with a quality good enough for the analysis. No perfect polishing nor etching is needed. The polishing time spent through all steps is almost one third of that used to be spent preparing the samples for the analysis with the

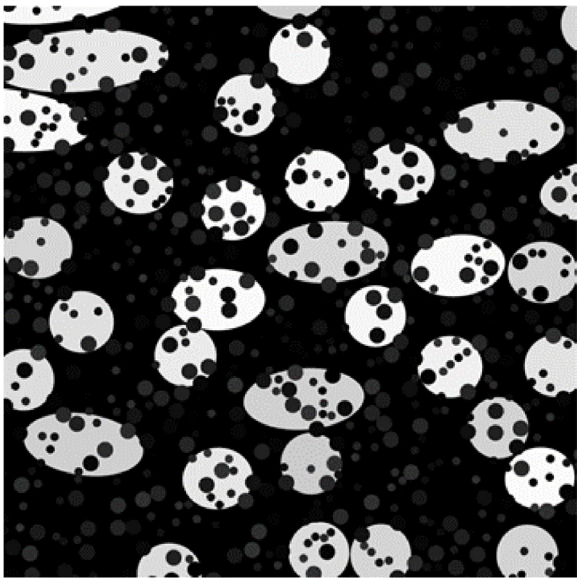

Fig. 3 An example of the synthetic training data for the network. The white ellipses mimic the fibres, the grey ellipses noise and the black background the matrix

conventional techniques. Sample preparations starts with a careful cut of the specimens using a diamond cutting disc, any small deviation in the cutting plane would induce other shapes for the fibre cross sections, thus wrong results after the ellipse fitting. Then, the polishing was carried out starting with rough polishing papers gradual to 9 μm, 6 μm and 3 μm diamond polishing suspensions. An example of the micrographs delivered after the sample preparation and ready for analysis using the new technique is shown in Fig. 2.

Fibre orientation measurements

The new proposed technique for image analysis makes the 2D fibre orientation measurement more accurate and faster, allows image treatment with polishing defects, with direct measurement without the need of image threshold or any corrections, and with better fitting of dense and crowd population of fibres. To enable automatic measurement of fibre angles in microscopy images a deep learning approach to image segmentation was developed using publicly available methods. A convolutional neural network architecture called Mask-RCNN ([28]) was applied to output instance segmented images. This means that for each fibre detected a binary pixel-mask is created. The implementation of Mask-RCNN from Detectron2 (https://github.com/facebookresearch/detectron2) was used to train the network and make predictions. There was no training data available for, for instance, segmented microscopy images of carbon fibres. Therefore 1000 synthetic images that mimics the microscopy images were generated. An example of a synthetic image can be seen in Fig. 3. The synthetic images were created by generating random white ellipses on a black background. These white ellipses represent the fibres. Then noise was added, to simulate scratches and imperfections, in the form of random grey ellipses. Binary masks of the white ellipses were also generated to be used as the ground truth data when training the model. The polishing defects, that are usually the reason behind the bad ellipse fitting, are taken into account. This consideration implies large time-savings later on in the image analysis since manual corrections are not required and since the program is trained with ML to deal with these defects so no perfect polishing will be required. First synthetic images were used, followed by training using real images, that makes the analysis using microscope pictures directly possible without the need for any threshold algorithm.

After training with the synthetic data, the network could output partially segmented images. These images were then manually annotated and corrected and used to retrain the network. The process as depicted in Fig. 4 was iterated until the output of the network was deemed acceptable.

Using the output from the network, first polygons and then ellipses were fitted to the pixel masks, output of this as well as resulting orientations can be seen in Fig. 5. The microscopy images had a resolution of 1920×1080

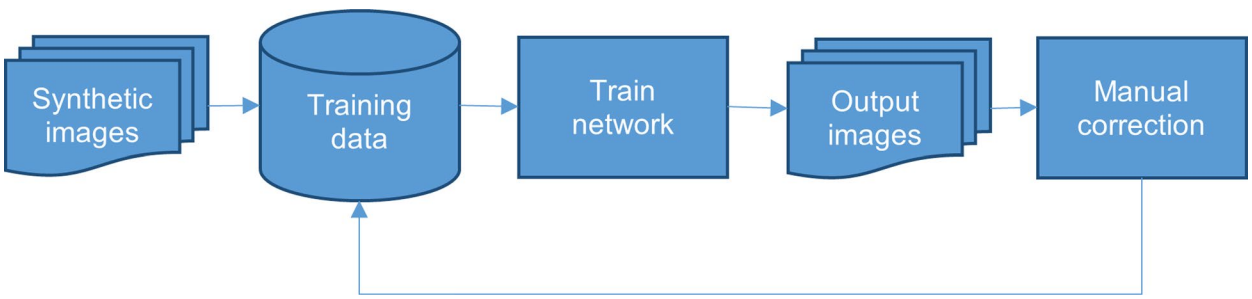

Fig. 4 Schematic view of the ML training process for the network

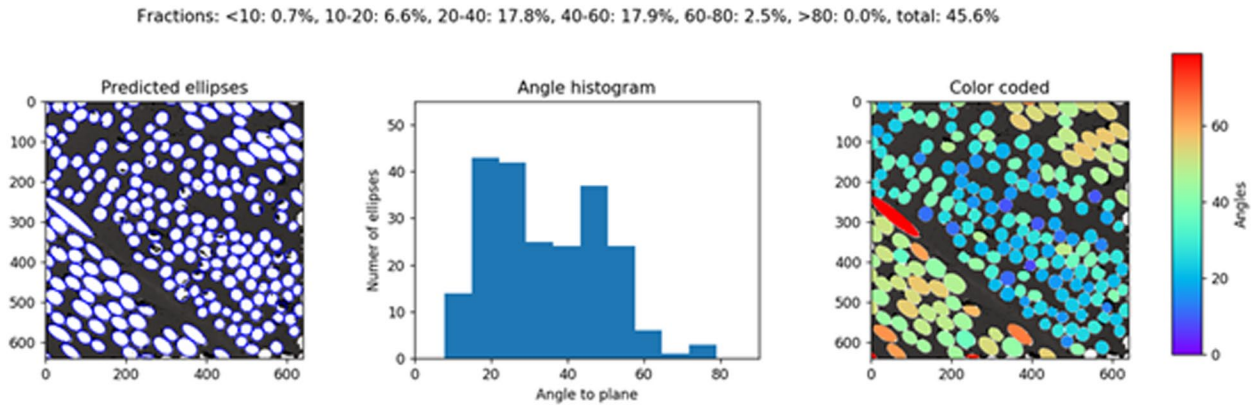

Fig. 5 From left to right: Ellipses (in blue) fitted to fibre masks on a polished cross-section (the white ellipses are the fibres), a histogram of ellipse angles with numbers of ellipses as a function of angle to the polished plane, and ellipses colour-coded according to the angle to the polished plane

pixels. Good results were harder to obtain when using the whole image and therefore 640×640 crops of the image are used. Using a sliding window, the whole image was processed with overlaps. The resulting polygons were merged before fitting ellipses. Long ellipses, obtained when the fibres are cut along or close to their longitudinal direction, still impose a challenge and especially if they are not horizontal in the image section and are close together. This could possibly be improved by implementing rotated bounding boxes for Mask-RCNN. There is also room for improvement in the merging of polygons.

Case setup

The pressing setup can be seen in Fig. 6. The geometry is a pressing tool used for rheological testing. The inner area (in dark grey in the left figure) indicates the initial charge placement with the initial charge having a diameter of 3.5 cm. The charge is pressed from an initial thickness of 2.86 mm to a final thickness of 0.36 mm.

To compare the numerical and experimental approaches, a plane is cut along the x-axis, this can also be seen in Fig. 5. The orientation tensors are measured at three locations: 10 mm from the left edge, at the midpoint and 10 mm from the right edge of the resulting disk respectively. These locations are marked in Fig. 6. Each of these windows have a width of 750 μm and cover the full height. For each of these windows 35 microscopy images are taken and used as a basis for the orientation tensor estimation.

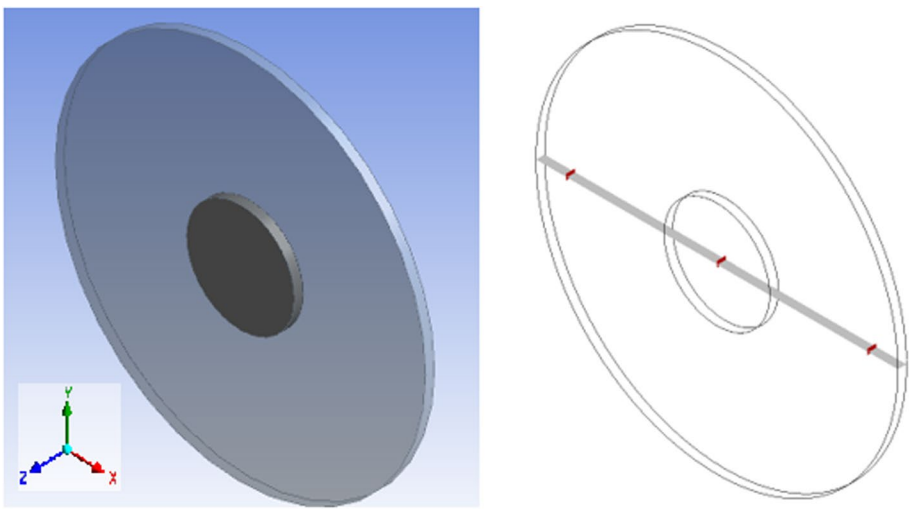

Fig. 6 A view of the press setup (rheological testing tool), along with the cutting plane used for the experimental measurements in which the specific measurement locations are marked in red. The initial charge, in dark grey in the left figure, has a diameter of 355 mm and initial charge height 2.86 mm

Results and discussion

Examples of the resulting fibre orientations from the experiments are displayed in Fig. 7, with one ML-analysed cross-section from each of the measurement windows. Coloured ellipses represent fibres that the image processing has managed to capture, and the colour scale is just used to distinguish the fibres from each other. Almost all fibres are coloured, meaning that the method can successfully capture orientation. It is worth noting that many of the fibres that are not coloured, i.e. not detected by the software, are as previously mentioned the more elongated ones that are more aligned with the flow direction, so a slight underprediction of the alignment with the flow direction is expected; however, since the fraction of non-coloured fibres is small, this error should not significantly affect the results.

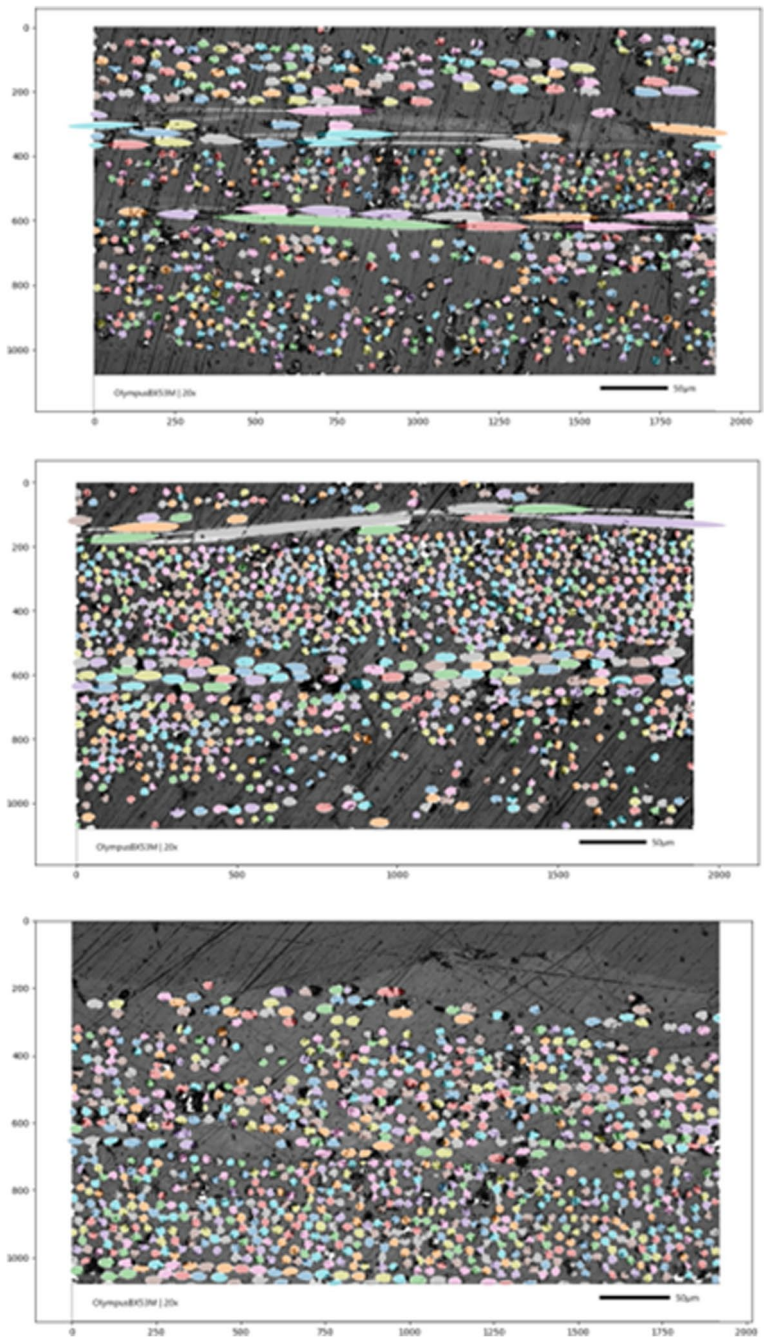

Fig. 7 Some examples of treated images where the fibres a coloured just to distinguish them from each other and to show that they are accounted for in the analysis. The grey area is the matrix. The upper example is from the left position, the middle from the middle position and the bottom from the right position respectively; consequently, the flow direction is to the left in the upper image and to the right in the bottom image

Orientation tensors from the two numerical methods as well as from the experimental results have been computed for three locations as described in the Case Setup section and as displayed in Fig. 5. In addition, measured thickness and area of the measurement windows of the SMC part can be seen in Table 1 for the three locations.

The resulting a_{11} and a_{22} tensors for the three positions are plotted in Figs. 8 and 9 respectively. Since the cut is along the x-axis, a_{11} is the component that is aligned with the principal flow direction, while a_{22} is perpendicular to the flow direction. Values of a_{11} and a_{22} equal to 0.5 means that the fibres are randomly oriented in the plane. Hence the 3DTimon simulations indicates that the flow do not influence the in-plane orientation to any larger extent although there is an element of alignment in the direction perpendicular to the flow direction. The Advani-Tucker approach in the 3D CFD case suggests that the fibres will align with the flow direction. However, for both the left and right cases results are still in a region where the orientation can be considered random. Regarding the comparison to the experimental data 3D Timon compares better but neither of the numerical methods predict the peak in orientation that occurs in Figs. 8 and 9 for the middle position. As can be seen in Table 1 the middle position is thinner than the other two positions. This is not currently captured in the numerical models used here. Additional experimental data would be required to study this effect. Other reasons to

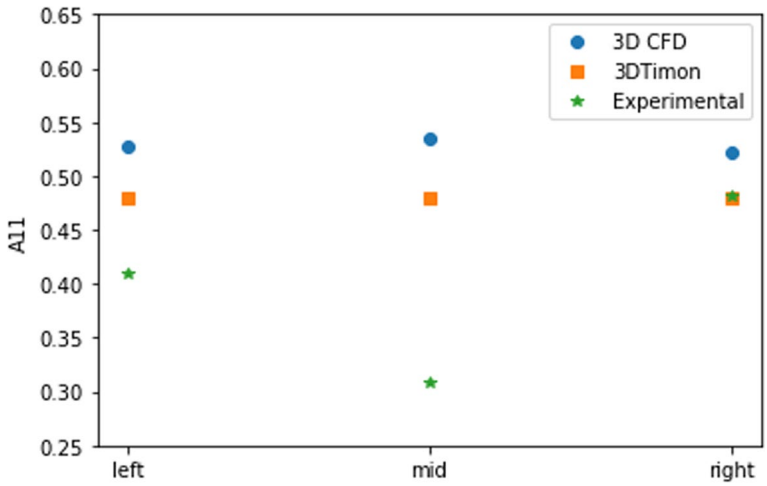

Fig. 8 Experimental and numerical results for the orientation tensor component aligned with the flow direction. Note that the scale is cut off in both the upper and lower end

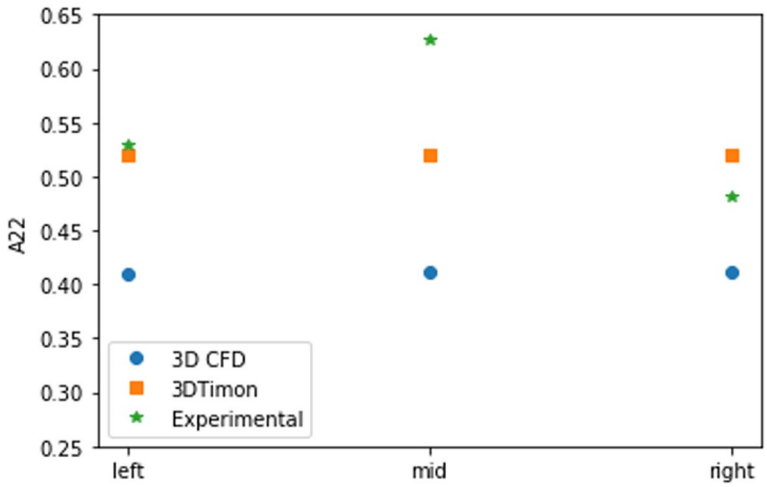

Fig. 9 Experimental and numerical results for the orientation tensor component perpendicular to the flow direction. Note that the scale is cut off in both the upper and lower end

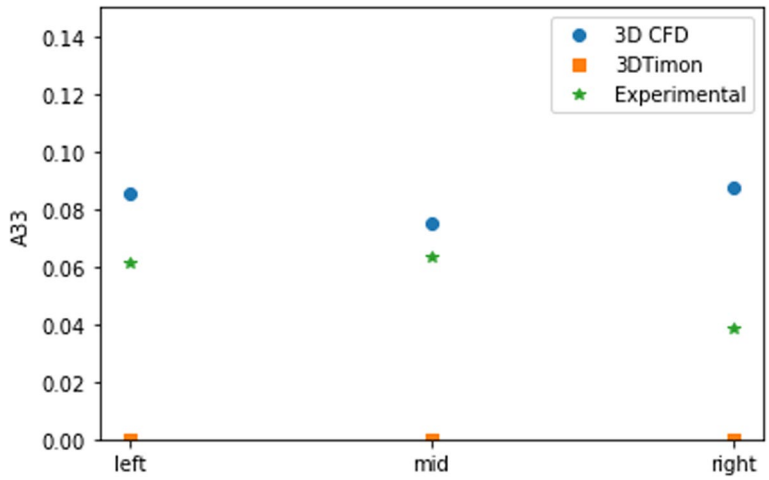

Fig. 10 Experimental and numerical results for the out-of-plane component of the orientation tensor. Note that the scale is cut off in the upper end

Table 1 Measured thickness of the sample SMC part at the three measurement windows

Position	Measured thickness [mm]	Measurement window [mm^2]
Left	0.36 ± 0.02	0.27 ± 0.015
Middle	0.27 ± 0.04	0.203 ± 0.03
Right	0.36 ± 0.015	0.27 ± 0.011

the discrepancies are that the Advani-Tucker approach for approximating fibre-fibre interactions was not developed for high fibre volume fraction materials as the one studied in this paper, and 3DTimon methodology applied does not take interactions into account. It would be expected that the high fibre volume fraction affects how the material behaves. It is, however, worth noting that the experimentally measured fibre orientations are still fundamentally random, so more experimental data are required in realizing whether there are any actual trends in the resulting orientations.

For the out-of-plane component, a_{33}, the 3D CFD approach and the experiments give results in the same direction, while 3DTimon predicts essentially no out-of-plane orientation whatsoever, see Fig. 10. Images from Odenberger et al. [29] and Olsson et al. [30] on the flow front and the motion of different layers, respectively, in real mouldings in a similar geometry as the one used here indicate that there should be an out-of-plane orientation of the fibres. Still more quantitative measurements are required to validate the predicted out-of-plane orientation.

Conclusions

Two numerical approaches for flow and fibres orientation modelling during compression moulding of a high fibre volume content SMC (35%) are presented. The fibre orientation results from the numerical simulations are compared to experimental results that are obtained using microscopy and a novel image recognition method based on describing the fibres in the images as ellipsoids and ML-algorithms. The image recognition software manages to capture almost all fibres and it is a much more efficient method as compared to a more manual process since less work is required to obtain microscope images with a quality good enough for the analysis. For the studied case, comparison between the experimental results and numerical methods indicate that simulations with 3D Timon show the largest randomness in principal and perpendicular flow direction, and hence less difference when compared to experiments at the outer edges of the circular disk. The 3D CFD approach shows larger resemblance with the experimental out-of-plane component. None of the numerical methods, however, manage to capture the unsymmetrical effects arising from the pressing and all in-plane results indicate a close to random orientation. Hence more experimental data is required to fully explore the trends in the resulting orientations and the models used for the simulations can be improved by for instance fully two-way or four-way coupled simulations.

Abbreviations

SMC Sheet Moulding Compound
A-SMC Advanced Sheet Moulding Compound

Authors' contributions

GA and YA preformed the numerical simulations with input from AL. HZ and EL developed the experimental method, and prepared Figs. 2, 3 and 4. GA provided the remaining figures. Manuscript was written by GA, HZ, AL and TSL. All authors reviewed the manuscript.

Funding

Open access funding provided by Lulea University of Technology. This work is a part of the PROSICOMP II project funded by the Swedish Research Innovation Agency (VINNOVA), through Lighter – a strategic innovation program funded by Vinnova, Swedish Energy Agency and Formas and FFI, Vehicle Strategic research and Innovation supported by Vinnova, the Swedish Transport Administration and the Swedish Energy Agency) and the automotive industry.

Availability of data and materials

The datasets generated and analyzed during this study are not publicly available due to licensing agreements with software providers but can be made available from the corresponding author on reasonable request.

Declarations

Competing interests

The authors declare no competing interests.

Received: 13 January 2023 Accepted: 25 October 2023
Published online: 20 November 2023

References

1. G. Alnersson, M.W. Tahir, A.L. Ljung, T.S. Lundström, Review of the numerical modeling of compression molding of sheet molding compound. Processes 8(2), 1–12 (2020)
2. L.J. Lee, L.F. Marker, R.M. Griffith, The rheology and mold flow of polyester sheet molding compound. Polym Compos 2(4), 209–218 (1981)
3. S. Le Corre, L. Orgeas, D. Favier, A. Tourabi, A. Maazouz, C. Venet, Shear and compression behaviour of sheet moulding compounds. Compos Sci Technol 62(4), 571–577 (2002)
4. S. Le Corre, D. Favier, P. Dumont, L. Orgeas, Anisotropic viscous behavior of sheet molding compounds (SMC) during compression molding. Int J Plast 19, 625–646 (2003)
5. P. Dumont, L. Orgeas, D. Favier, P. Pizette, C. Venet, Compression moulding of SMC: in situ experiments, modelling and simulation. Compos Part A: Appl Sci Manufac 38(2), 353–368 (2007)
6. Vahlund FC, Gebart RB. Squeeze flow rheology in large tools. In: Proceedings of the 5th International Conference on Flow Processes in Composite Materials, Plymouth, UK. 1999. p. 365-372.
7. MR. Barone, DA. Caulk, Kinematics of flow in sheet molding compounds. Polymer composites 6(2), 105–9 (1985)
8. Olsson, N. E. J., Lundström, T. S., & Olofsson, K. (2009). Design of experiment study of compression moulding of SMC. Plastics, rubber and composites, 38(9-10), 426-431.
9. F. Folgar, C.L. Tucker, Orientation behavior of fibers in concentrated suspensions. J Reinf Plast Compos 3(2), 98–119 (1984)
10. S.G. Advani, C.L. Tucker, The use of tensors to describe and predict fiber orientation in short fiber composites. J Rheol 31(8), 751–784 (1987)
11. J. Wang, J.F. O'Gara, C.L. Tucker, An objective model for slow orientation kinetics in concentrated fiber suspensions: theory and rheological evidence. J Rheol 52(5), 1179–1200 (2008)
12. H.C. Tseng, R.Y. Chang, C.H. Hsu, Phenomenological improvements to predictive models of fiber orientation in concentrated suspensions. J Rheol 57(6), 1597–1631 (2013)
13. H.C. Tseng, R.Y. Chang, C.H. Hsu, An objective tensor to predict anisotropic fiber orientation in concentrated suspensions. J Rheol 60, 215–224 (2016)
14. G. Alnersson, TS. Lundström, A-L. Ljung. Numerical study of the 3D-flow characteristics during compression moulding of SMC. In: 22nd International Conference on Composite Materials (ICCM22), Melbourne, Australia, August 11-16, 2019. RMIT University, 2019. p. 1571-1581.
15. M. Kobayashi, K. Dan, T. Baba, D. Urakami, Compression molding 3D-Cae of discontinuous long fiber reinforced polyamide 6: Influence on cavity filling and direct fiber simulations of viscosity fitting methods. 20th International Conference on Composites Materials 19, 1–12 (2015)
16. YA. Cengel, JM. Cimbala. Fluid Mechanics: Fundamentals and Applications. 3rd ed. McGraw-Hill, New York, NY; 2014.
17. N.E.J. Kluge, T.S. Lundström, L.G. Westerberg, K. Olofsson, Compression moulding of sheet moulding compound: modelling with computational fluid dynamics and validation. J Reinf Plast Compos 34(6), 479–492 (2015)
18. M. Sepehr, P.J. Carreau, M. Moan, G. Ausias, Rheological properties of short fiber model suspensions. J Rheol 48(5), 1023–1048 (2004)
19. S.M. Högberg, H.O. Åkerstedt, T.S. Lundström, J.B. Freund, Respiratory deposition of fibers in the non-inertial regimedevelopment and application of a semi-analytical model. Aerosol Sci Technol 44(10), 847–860 (2010)
20. S.G. Advani, C.L. Tucker, Closure approximations for three-dimensional structure tensors. J Rheol 34(3), 367–386 (1990)
21. G.L. Hand, A theory of anisotropic fluids. J Fluid Mech 13(1), 33–46 (1962)
22. C. Eberhardt, A. Clarke, Fibre-orientation measurements in short-glass-fibre composites. Part I: automated, high-angular-resolution measurement by confocal microscopy. Compos Sci Technol 61(10), 1389–1400 (2001)
23. C. Eberhardt, A. Clarke, M. Vincent, T. Giroud, S. Flouret, Fibre-orientation measurements in short-glass-fibre composites — part II: a quantitative error estimate of the 2D image analysis technique. Compos Sci Technol 61(13), 1961–1974 (2001)
24. N.D. Sharp, J.E. Goodsell, A.J. Favaloro, Measuring fiber orientation of elliptical fibers from optical microscopy. J Compos Sci 2019;3(1).
25. A.R. Clarke, G. Archenhold, N.C. Davidson, A novel technique for determining the 3D spatial distribution of glass fibres in polymer composites. Compos Sci Technol 55(1), 75–91 (1995)
26. B. Mlekusch, E.A. Lehner, W. Geymayer, Fibre orientation in short-fibre-reinforced thermoplastics I. contrast enhancement for image analysis. Compos Sci Technol 59(4), 543–545 (1999)
27. G.M. Velez-Garc´ıa, P. Wapperom, V. Kunc, D.G. Baird, A. Zink-Sharp, Sample preparation and image acquisition using optical-reflective microscopy in the measurement of fiber orientation in thermoplastic composites. J Microsc 248(1), 23–33 (2012)
28. K. He, G. Gkioxari, P. Doll'ar, R. Girshick, Mask R-CNN. IEEE Trans Pattern Anal Mach intell 42(2), 386–397 (2020)
29. P.T. Odenberger, H.M. Andersson, T.S. Lundstr√∂m, Experimental flow-front visualisation in compression moulding of SMC. Composites Part A 32, 1125–1134 (2004)
30. N.E.J. Olsson, T.S. Lundström, K. Olofsson, A design of experimental study of compression moulding of SMC plastics. Rubber Composites 38(9/10), 428–433 (2009)

Publisher's Note